Development of Transport Model in Reactor Plasmas based on LHD Experiment Scaling*)

Ryosuke SEKI, Masahiko SATO, Kiyomasa WATANABE, Hisamichi FUNABA, Yasuhiro SUZUKI, Satoru SAKAKIBARA, Atsushi FUKUYAMA[1)], Sadayoshi MURAKAMI[1)] and Noriyoshi NAKAJIMA

National Institute for Fusion Science, Toki 509-5292, Japan
[1)]*Graduate School of Engineering Kyoto University, Kyoto 606-8501, Japan*

(Received 9 December 2012 / Accepted 16 April 2013)

We propose a transport model based on a systematic analysis of local transport for a large number of Large Helical Device discharges. This model allows us to more accurately predict the plasma performance compared with early researches in the helical plasmas. The proposed model has been applied to the integrated modeling code, TASK3D. We have developed a code to predict the confinement performance in the reactor-relevant high-beta regime. In the predictions of high-beta discharges maintained by NBIs, when field strength increases from 0.43 T to 0.9 T, the achievable beta value decreases by about 1%, but the magnetic Reynolds number increases about 10 times larger. In the prediction to add the perpendicularly NBs with the "re-entering fast ion" effect, the achievable beta value increase by about 0.3%. On the other hand, the magnetic Reynolds number barely changes.

Keywords: transport model, prediction, high beta, LHD, re-entering fast ion

DOI: 10.1585/pfr.8.2403089

1. Introduction

In the Large Helical Device (LHD), reactor-relevant high-beta plasmas with volume-averaged beta ($\langle\beta\rangle$) of ~ 5% are achieved without disruptive phenomena. The LHD high-beta discharge is maintained in a steady state for longer than the energy relaxation time [1]. The helical type device like the LHD has an advantage in a steady operation, which is important for an efficient fusion reactor, because the helical type device does not require the plasma current for making the magnetic field. However, for LHD high-beta plasma, the typical gyro radius normalized by the minor radius and the collision frequency are larger than for the reactor by factors of about ten and sixty, respectively. There are the large gaps of plasma parameters between the LHD high beta plasma and the helical type reactor. Therefore, the establishment of integrated physics model is required to bridge over the gap for the design of the fusion reactor.

To predict the plasma confinement performances of a LHD-type fusion reactor, the integrated transport code TASK3D [2] is being developed for three-dimensional configurations. TASK3D is primarily based on a transport simulation that combines various simplified models that describe physical processes in different hierarchies. It is an extension of the integrated transport code TASK (transport analyzing system for tokamaks) for tokamak plasmas [3], which was developed at Kyoto University. In the TASK3D, MHD models and transport modes are extended to include the three-dimensional effect.

Experimental results indicate that the plasma confinement performance in the core plasma of the fusion reactor is mainly determined by transport due to turbulence, which is called "anomalous transport." In the LHD, a number of theoretical anomalous transport models have been proposed. To date, no theoretical anomalous transport model can fully describe the local transport property in the LHD high-beta plasma. Therefore, we propose a local transport model based on a systematic local transport analysis of a large number of LHD discharges in order to predict the reactor plasma. In this paper, the proposed transport model is applied to the TASK3D and the confinement performance in the high beta regime is predicted.

2. Transport Model for High-Beta Plasmas Based on LHD Experiment Scaling

The local thermal conductivity for many LHD high beta discharges is systematically analyzed on the basis of the power balance in the case of the diffusion-type transport model (i.e., the heat flux is proportional to the thermal conductivity and the temperature gradient). From these local transport analyses, we propose a local thermal transport model. The model would enables more accurate predictions of the characteristics of LHD-type reactor plasmas because it considers the transport properties in the reactor-relevant high-beta regime of LHD-type reactors.

author's e-mail: seki.ryohsuke@lhd.nifs.ac.jp
*) This article is based on the presentation at the 22nd International Toki Conference (ITC22).

Firstly, the thermal transport properties in the low-beta regime of the LHD are described. In the LHD, the global confinement time is scaled as the ISS04 scaling [4], which has the similar dependency of the gyro-Bohm model. In addition, local transport analyses [5] indicate that the dependence of the local thermal conductivity is very similar to that of the ISS04 model. The local thermal conductivity is expressed by introducing the form factor C_χ to the ISS04 model as follows:

$$\chi_{\mathrm{ISS04}} = C_\chi \beta^{0.19} \nu_*^{0.00} \rho_*^{0.79} A_p^{-0.07} \iota_{2/3}^{-1.06} \chi^{\mathrm{Bohm}}, \quad (1)$$

where χ^{Bohm} comes from the Bohm-type transport model and ρ_*, β, ν_*, A_p and ι are the local normalized Larmor radius, the local beta value, the local normalized collision frequency, the aspect ratio, and the rotational transform, respectively. Here C_χ is approximated by a polynomial equation with a minor radius based on the local transport analyses.

Next, we discuss the transport properties in the high-beta regime. In a LHD high-beta discharge, an increase in β results in a gradual degradation of the confinement performance. The local transport analysis of high-beta discharges shows that the local thermal conductivity increases in the peripheral region (normalized minor radius $\hat{r} \sim 0.9$) [6]. Here the local thermal conductivities are analyzed in the region of the nested magnetic flux surface predicted by the HINT code [7, 8]. Therefore, transport degradation within $\hat{r} \sim 0.9$ may not be mainly caused by the stochastization of the nested magnetic flux surface. On the other hand, the resistive interchange mode (g-mode) is unstable in the peripheral region, and consistent long-wave fluctuations are measured. The local thermal conductivity in the peripheral region is found to have the same dependency on the resistive interchange MHD instability in the driven anomalous model [9] g-mode:

$$\chi_{\mathrm{GMTe}} \propto \beta^{1} \nu_*^{0.67} \rho_*^{0.33} \chi^{\mathrm{Bohm}}. \quad (2)$$

Based on these transport properties of high-beta plasma, we propose the following transport model that incorporates the ISS04 type and g-mode turbulence (GMT) type anomalous transport models in addition to the neoclassical transport model:

$$\chi_{\mathrm{s}} = \chi_{\mathrm{CHs}} + \chi_{\mathrm{SHs}} + c_{1\mathrm{s}} * \chi_{\mathrm{ISS04s}} + c_{2\mathrm{s}} * \chi_{\mathrm{GMTs}}, \quad (3)$$

where χ_{CHs} and χ_{SHs} are the axisymmetric and nonaxisymmetric parts of the neoclassical transport. $c_{1\mathrm{s}}$ and $c_{2\mathrm{s}}$ are the constants with the order of unity so as to well reproduce the experimental temperature profiles. The plasma species is denoted by s. In the transport analyses referred to above, the effective thermal conductivity, which is defined as the average of the electron and ion thermal conductivities, is evaluated on the basis of an assumption that the ion temperature and density are the same as the electron temperature and density, because a main component of ion heating is the thermal transition from electrons to ions, and the number of the measurement of the ion temperature have been much smaller in the high beta discharge. However, in our model, χ_{e} and χ_{i} are needed to reproduce the temperatures; thus, $c_{1\mathrm{s}}$ and $c_{2\mathrm{s}}$ must be determined. The value of $c_{2\mathrm{s}}$ for χ_{GMT} can be determined from the resistive interchange MHD instability-driven anomalous model. The value $c_{1\mathrm{s}}$ for χ_{ISS04} is selected to reproduce the temperature of the experimental plasma. In our model, assuming that the ion temperature of the experimental plasma approximately equals the electron temperature, $c_{1\mathrm{e}} \sim 1.88$, $c_{1\mathrm{i}} \sim 0.17$, $c_{2\mathrm{e}} \sim 1.0$, and $c_{2\mathrm{i}} \sim 1.0$ are determined to be appropriate for discharges with 0.9 T, $\langle\beta\rangle \sim 2.7\%$, $n_{\mathrm{e}} \sim 3 \times 10^{19}\ \mathrm{m}^{-3}$, and 0.425 T, $\langle\beta\rangle \sim 4.5\%$, $n_{\mathrm{e}} \sim 4 \times 10^{19}\ \mathrm{m}^{-3}$. In LHD high-beta plasmas, the ion temperature of the experimental plasma may roughly equal the electron temperature because the plasma relaxation time is very short. Analysis and modeling of ion transport in LHD high beta discharges are issues for future study.

3. Prediction Code of Confinement Performance in High Beta Discharge

We introduced the transport model discussed in Section 2 into TASK3D and implemented a function to predict the confinement performance in the high-beta regime. The flow chart of the prediction code of the confinement performance is shown in Fig. 1. A TR module [3] of the TASK3D, in which the heat flux is expressed by the diffusion formula, is used to calculate the temporal development of the plasma temperature and the density. We applied the proposed transport model to the TR module.

In this code, the equilibrium magnetic field is calculated by the VMEC and the heating power profile is evalu-

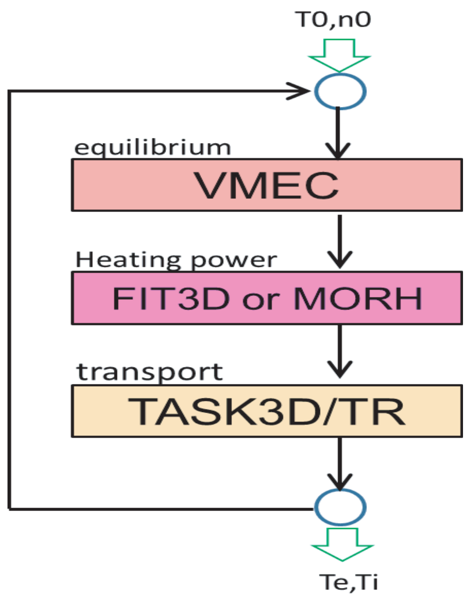

Fig. 1 Flow chart of prediction code of confinement performance.

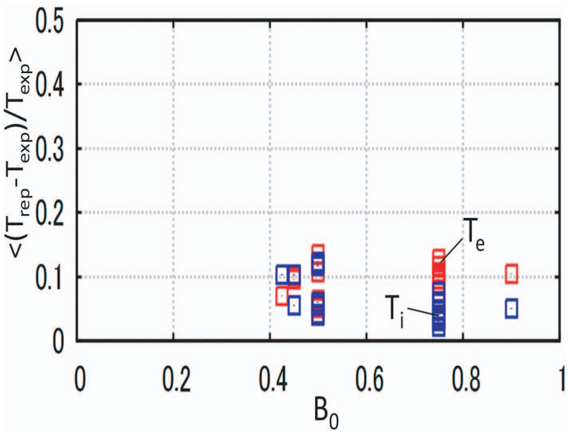

Fig. 2 Relative errors of reproduced temperatures. The horizontal axis denotes the field strength of high beta discharge and the vertical axis is the average of the relative error of the reproduced electron temperature.

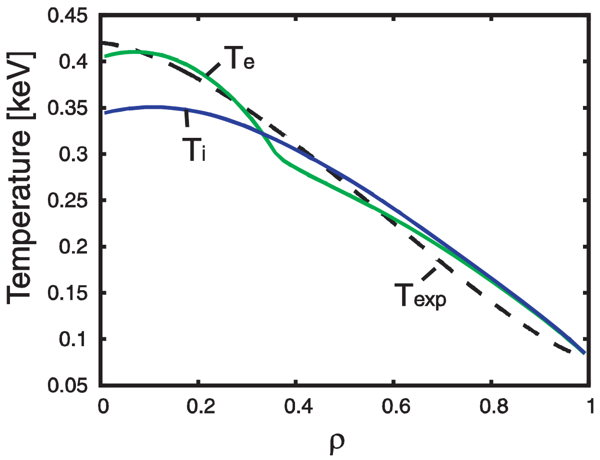

Fig. 3 Profiles of reproduced electron and ion temperatures for high-beta plasma with B_0 = 0.43 T. The dashed line shows the electron temperature measured in LHD experiments. The blue and green lines are the reproduced ion and electron temperatures, respectively.

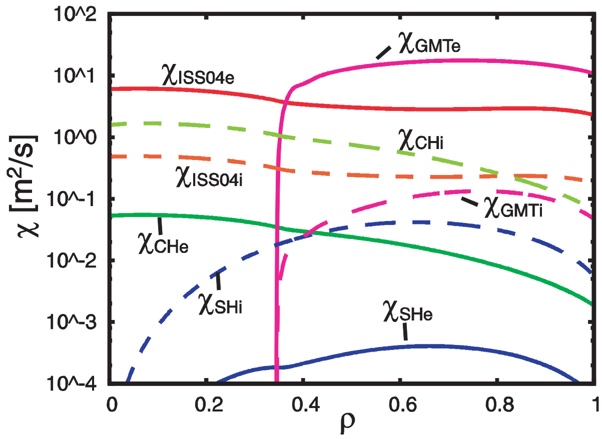

Fig. 4 Components of thermal conductivity in reproduced plasma with B_0= 0.43 T. The solid and dashed lines denote the electron and ion thermal conductivities, respectively. The red, purple, green, and blue lines show χ_{ISS04}, χ_{GMT}, χ_{CH}, χ_{SH}, respectively.

ated by FIT3D [10] or MORH [11] for the each time step shown in Fig. 1. Here FIT3D is a simple code to evaluate neutral beam injection (NBI) heating power, and the MORH is a Monte Carlo code based on orbits following in real coordinates. In the proposed code, the density is not calculated, and its profile corresponds to a typical profile for LHD high-beta plasmas. Furthermore, the code applies an iterative calculation until the changes in temperature and stored energy are sufficiently small. Finally, the predicted temperature profile is evaluated.

To test the validity of our model before using it for predictions, we reproduced LHD high-beta plasma. Figure 2 shows the relative errors of calculated temperatures. For the LHD high-beta plasma, the relative errors of the electron temperature are around 10%. This result indicates that the proposed transport model can reproduce the experimental electron temperature. In addition, the reproduced ion temperatures also have a relative error of around 10%. The assumption that the ion temperature approximately equals the electron temperature is satisfied.

Figure 3 shows the reproduced profile of the electron and ion temperatures for high-beta plasma with B_0 = 0.43 T. The broken line is the measured electron temperature (the ion temperature was not measured in this case). The calculated profile of the electron temperature is almost the same as the experimental profile. The components of the thermal conductivity in the reproduced plasma are shown in Fig. 4. In the reproduced plasma, the resistive interchange instability-driven anomalous transport dominates the electron thermal transport, and the neoclassical transport dominates the ion transport.

4. Prediction of LHD High-Beta Plasma Closer to the Fusion Reactor

The transport model based on the present high beta discharges might not be sufficiently accurate to predict the fusion reactor plasmas because the parameter gap between the LHD present high beta plasmas and the reactor ones is fairly large. To improve the accuracy of the extrapolation, the differences in plasma parameters between LHD high-beta plasmas and reactor plasmas should be decreased. Thus, to improve our proposed transport model, high-beta discharge plasmas with higher fields are required because their plasma parameters are closer to those of a LHD-type fusion reactor. In addition, in LHD high-beta plasmas, the confinement performance is degraded because of the resistive interchange mode. The resistive interchange mode may be inhibited by increasing the magnetic Reynolds number which increases as the field strength and the temperature increases. This instability should be inhibited to achieve plasma parameters close to those of a LHD-

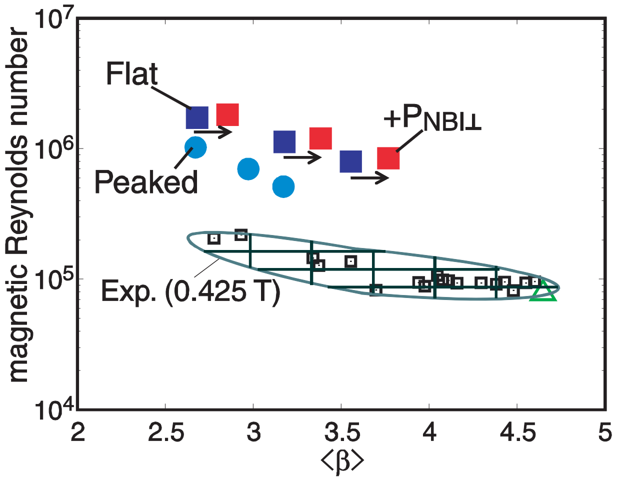

Fig. 5 Components of thermal conductivity in reproduced plasma with B_0 = 0.43 T. The solid and dashed lines denote the electron and ion thermal conductivities, respectively. The red, purple, green, and blue lines show χ_{ISS04}, χ_{GMT}, χ_{CH}, χ_{SH}, respectively.

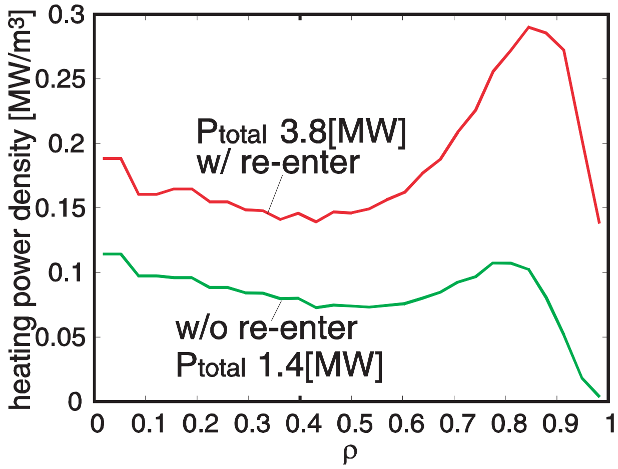

Fig. 6 Components of thermal conductivity in reproduced plasma with B_0 = 0.43 T. The solid and dashed lines denote the electron and ion thermal conductivities, respectively. The red, purple, green, and blue lines show χ_{ISS04}, χ_{GMT}, χ_{CH}, χ_{SH}, respectively.

type fusion reactor. This is important to accurately predict the magnetic Reynolds number for high beta plasma under higher field strength.

Therefore, we used the code developed to investigate an optimized operational condition in a regime with higher magnetic field (B_0 = 0.9 T) than for the present high-beta discharge. Figure 5 shows the expected operation regime in terms of $\langle\beta\rangle$ and magnetic Reynolds number for ρ = 0.5. The hatched region corresponds to the operational conditions of a typical high-beta discharge. The solid blue circles represent the predicted operational regime at 0.9 T with a tangentially injected NBI at 15 MW port-through power, which corresponds to the maximum heating power in the hatched region. Here the average density changes, and the squares and circles denote the flat and peaked density cases, respectively. For the same average density, the flat density profile is favorable to push up the magnetic Reynolds number. Note that, in the hatched region with B_0 = 0.43 T, the typical density profile is flat. Based on Fig. 5, an increase in B_0 from 0.425 to 0.9 T results in a decrease in the achievable $\langle\beta\rangle$ from 4.7% to 3.5%, but the magnetic Reynolds number increases by an order of magnitude at $\langle\beta\rangle \sim 3.5\%$.

Next, we discuss the operation regime with perpendicularly injected NBs and tangentially injected NBs. For the high-beta discharge, most of the trapped particles produced by perpendicularly-NBs pass out of the last closed flux surface (LCFS) because of the large deviation between the orbits and the flux surfaces, and some of them are not lost and can re-enter in the region of the closed flux surfaces, which is called "re-entering fast ion" [12]. Therefore, the effect of the re-entering fast ion should be included to accurately evaluate the heating power profile. Figure 6 shows the heating power profile with and without re-entering effects by using the MORH code and for the case of the available LHD port-through NBI powers (12 MW, $\langle\beta\rangle \sim 3.5\%$). In Fig. 6, when the re-entering fast ions are considered, the effective heating power of the perpendicularly injected NB is around 2.5 times as large as that obtained without considering the re-entering effect. By considering the perpendicularly injected NB and the re-entering effect (shown by red squares in Fig. 5), the achievable $\langle\beta\rangle$ in the expected operation regime increases by around 0.2%, whereas the magnetic Reynolds number changes barely. However, analysis of Fig. 6 shows that the effective heating power is around a third of the port-through power even when the re-entering effect is included. This result is because of the fact that most of the particles produced by the perpendicularly injected NB become chaotic orbit particles [12] and are lost because of the low field. In the future, we plan to investigate the field strength dependency of the heating efficiency of the perpendicular injected NB and to find the most suitable field strength for maintaining the high-beta discharge.

5. Summary

We propose a transport model based on systematic local transport analyses. The proposed model is used to develop a code to predict the confinement performance for reactor-relevant high-beta and collision less regimes. The model was applied to the integrated modeling code, TASK3D. It is confirmed that the proposed model almost reproduces the electron temperature measured in the high beta discharge and satisfies the assumption the ion temperature approximately equals the electron temperature. In addition, to achieve a high-beta discharge with parameters closer to the plasma parameters of a LHD fusion reactor, we investigate an optimized operational condition in the higher-field regime. By increasing the field strength from

0.425 to 0.9 T, beta decreases from 4.7% to 3.5%, but the magnetic Reynolds number, which is the index of the inhibition of the transport degradation due to the resistive interchange mode, increases by an order of magnitude. If we add perpendicularly injected NBs, the beta is predicted to increase by around 0.3%, but the magnetic Reynolds number changes barely.

For the previous transport analyses in which our transport model used, we assumed that ion temperature equaled electron temperature because the number of the measurement of the ion temperature had been much smaller in the high beta discharge. In recent years, the number of measurements of ion temperature in high-beta plasmas has increased. We will analyze the properties of the thermal conductivities of ions and electrons by using the code TASK4LHD [13]. Based on these experimental results, a more accurate transport model will be developed.

[1] H. Yamada *et al.*, Nucl. Fusion **51**, 094021 (2011).
[2] A. Wakasa *et al.*, Proc. of 23rd IAEA Fusion Energy Conf., (Daejeon, Korea, 2010) THC/P4-29.
[3] A. Fukuyama *et al.*, Proc. of 20th IAEA Fusion Energy Conf., (Villamoura, Portugal, 2004) IAEA-CSP-25/CD/TH/P2-3.
[4] H. Yamada *et al.*, Nucl. Fusion **45**, 1684 (2005).
[5] H. Funaba *et al.*, Plasma Fusion Res. **3**, 022 (2008).
[6] K.Y. Watanabe *et al.*, Phys. Plasmas **18**, 056119 (2011).
[7] T. Hayashi, Theory of Fusion Plasmas, EUR 12149 EN 11 (1989).
[8] K. Harafuji, T. Hayashi and T. Sato, J. Comput. Phys. **81**, 169 (1989).
[9] B.A. Carreras and P.H. Diamond, Phys. Fluids B **1**, 1011 (1989).
[10] S. Murakami *et al.*, Trans. Fusion Technol. **27**, 256 (1995).
[11] R. Seki *et al.*, Plasma Fusion Res. **5**, 027 (2010).
[12] R. Seki *et al.*, Plasma Fusion Res. **3**, 016 (2008).
[13] R. Seki *et al.*, Plasma Fusion Res. **6**, 240481 (2011).